



Intercomparison of multi-GNSS signals characteristics acquired by a low-cost receiver connected to various low-cost antennas

Grzegorz Marut¹ · Tomasz Hadas¹ · Jakub Nosek^{2,3}

Received: 15 November 2023 / Accepted: 15 February 2024 / Published online: 8 March 2024
© The Author(s) 2024, corrected publication 2024

Abstract

With the increasing number of low-cost GNSS antennas available on the market, there is a lack of comprehensive analysis and intercomparison of their performance. Moreover, multi-GNSS observation noises are not well recognized for low-cost receivers. This study characterizes the quality of GNSS signals acquired by low-cost GNSS receivers equipped with eight types of antennas in terms of signal acquisition, multipath error and receiver noise. The differences between various types of low-cost antennas are non-negligible, with helical antennas underperforming in every respect. Compared with a geodetic-grade station, GPS and Galileo signals acquired by low-cost receivers are typically weaker by 3–9 dB-Hz. While the L1, E1 and E5b signals are well-tracked, only 72% and 86% of L2 signals are acquired for GPS and GLONASS, respectively. The signal noise for pseudoranges varies from 0.12 m for Galileo E5b to over 0.30 m for GLONASS L1 and L2, whereas for carrier-phase observations it oscillates around 1 mm for both GPS and Galileo frequencies, but exceeds 3 mm for both GLONASS frequencies. Antenna phase center offsets (PCOs) vary significantly between frequencies and constellations, and do not agree between two antennas of the same type by up to 25 mm in the vertical component. After a field calibration of a low-cost antenna and consistent application of PCOs, the horizontal and vertical accuracy is improved to a few millimeter and a few centimeter level for the multi-GNSS processing with double-differenced and undifferenced approach, respectively. Last but not least, we demonstrate that PPP-AR is possible also with low-cost GNSS receivers and antennas, and improves the precision and convergence time. The results prove that selection of low-cost antenna for a low-cost GNSS receiver is of great importance in precise positioning applications.

Keywords Low cost · Antenna · Phase center offset · Receiver noise · Positioning performance

Introduction

Global navigation satellite systems (GNSS) significantly impact geodesy and surveying fields, including precise positioning (Correa Muñoz and Cerón-Calderón 2018), surface deformations (Martín et al. 2015), ionosphere (Yasyukevich et al. 2020) and troposphere remote sensing (Vaquero-Martínez and Antón 2021), tectonic plate motion monitoring (Jagoda 2021) as well as landslide monitoring (Komac et al. 2015) or seismology (Nie et al. 2016). Despite results even at the submillimeter level, the primary limitation to the use of GNSS in various geoscience applications is the cost of the geodetic-grade receivers with associated high-precision antennas along with a high risk of damage or theft. With the emergence of low-cost GNSS receivers on the market, the cost of surveying with satellite techniques falls dramatically, while work begins on the possibilities of using low-cost receivers in novel geoscience applications.

✉ Tomasz Hadas
tomasz.hadas@upwr.edu.pl

Grzegorz Marut
grzegorz.marut@upwr.edu.pl

Jakub Nosek
jakub.nosek@pecny.cz

¹ Institute of Geodesy and Geoinformatics, Wrocław University of Environmental and Life Sciences, C. K. Norwida 25, 50-375 Wrocław, Poland

² Institute of Geodesy, Brno University of Technology, Antonínská 548/1, 601 90 Brno, Czech Republic

³ Research Institute of Geodesy, Topography and Cartography, Ústecká 98, 250 66 Zdíby, Czech Republic

Current research indicates the high potential of low-cost GNSS receivers, both single and dual frequency, in positioning (Wielgocka et al. 2021), displacement detection (Biagi et al. 2016; Hamza et al. 2021a), deformation monitoring (Cina and Piras 2015), vehicle navigation (Skoglund et al. 2016), autonomous agriculture (Han et al. 2017), as well as atmospheric studies (Kriemeyer et al. 2020). However, they still show deficiencies compared to geodetic receivers. The commonly used dual-frequency u-blox ZED-F9P chipsets are characterized by high sensitivity to signals reflected and degraded by the environment, up to -160 dB, which simultaneously translates into increased vulnerability to the multipath effect (Romero-Andrade et al. 2021b) and a weaker signal of about 7 dB-Hz recorded by the devices compared to high-end receivers, especially for signals coming from satellites at lower elevation angles (Wielgocka et al. 2021). However, the lower-quality weaker signal recorded by low-cost devices still provides satisfactory results that can complement professional high-end geodetic receivers to densify existing monitoring networks for GNSS meteorology (Marut et al. 2022). Kazmierski et al. (2023) found that utilizing observation networks comprising both low-cost and professional GNSS receivers enable the attainment of accuracies of 17 mm and 40 mm in the horizontal and vertical components, respectively. Bojorquez-Pacheco et al. (2023) achieved mm to cm level precision of horizontal coordinates using low-cost receivers for static relative positioning. Moreover, it is shown that low-cost receivers meet the ISO-17123-8 standard for measurements performed using the real-time kinematic (RTK) technique, with position determination uncertainties at the level of 5.5 mm and 11.0 mm, respectively, horizontally and vertically (Garrido-Carretero et al. 2019). RTK positioning allows for the use of low-cost GNSS receivers in traditional cadastral measurements (Wielgocka et al. 2021; Hamza et al. 2023). The accuracy of the obtained final Zenith Total Delay (ZTD) at the level of 4 mm (Kriemeyer et al. 2020) legitimates these devices for meteorological projects such as E-GVAP (<http://egvap.dmi.dk/>). The potential of low-cost GNSS devices in tropospheric studies is further confirmed by the high precision of the determined integrated water vapor (IWV) at the level of 0.3 kg/m² compared to a collocated water vapor radiometer (Marut et al. 2022). The analyses also show a high agreement of GNSS measurements performed with both low-cost and geodetic receivers, aligning with the ERA5 tropospheric model to an accuracy level of up to 10 mm (Stępnik and Paziewski 2022).

At the same time as testing the potential of low-cost GNSS receivers, the scientific community seeks ways to overcome their limitations. Takatsu and Yasuda (2008) suggest replacing the low-cost patch antenna with one of better specifications. Hamza et al. (2021b) confirm that the use of at least survey-grade antennas allows positioning with

accuracy of single millimeters under favorable measurement conditions and detecting displacements larger than 4 mm. However, under less favorable urban conditions, replacing the antenna, even with a geodetic-grade antenna, does not significantly improve the results due to the high vulnerability of the receiver to registering reflected and degraded signals (Hamza et al. 2023). In addition to replacing the antenna, it is also recommended to extend the measurement period and increase the sampling frequency to 1 s (Romero-Andrade et al. 2021a). A noticeable improvement is also achieved by using circular ground planes, which limit the registration of reflected signals. Zhang and Schwieger (2018) propose a choke-ring ground planes dedicated to low-cost antennas, which improve the obtained results by 50% and 35%, respectively, compared to results for antennas without any ground planes and with a flat ground plane without a choke-ring. Paziewski et al. (2019) suggest changing the stochastic model by altering the observation weighting scheme, e.g., using the signal-to-noise (SNR) ratio-based approach for smartphone positioning, which improves coordinate precision by up to 40%. Kriemeyer et al. (2022) notice that results obtained with low-cost antennas are affected by the lack of antenna calibration models, i.e., phase center offsets (PCO) and phase center variations (PCV). The application of individual calibration methods established for geodetic antennas would significantly increase the cost of low-cost GNSS devices. A field method for GPS, PCO and PCV determination reduces the error of the height component by half (Kriemeyer et al. 2022). Odolinski and Teunissen (2020) propose replacing the classical ambiguity resolution (AR) approach in relative positioning with the best integer equivariant (BIE) estimation, which allows for obtaining at least the same results as in the common AR approach.

Despite many recent advancements in low-cost GNSS, some topics still remain open. With the increasing number of low-cost antennas available on the market, there is a lack of comprehensive analysis of their performance, including vulnerability to multipath, repetitiveness of PCO/PCV models or their agreement with models provided by the manufacturer. Multi-GNSS observation noises are not well recognized for low-cost receivers, even though this knowledge may significantly contribute to the redefinition of the stochastic model. Moreover, it has not been yet confirmed if Precise Point Positioning-Ambiguity Resolution (PPP-AR) is possible with low-cost GNSS surveying equipment.

The goal of this study is to further characterize the quality of GNSS signals acquired by low-cost GNSS receivers equipped with various antennas. Therefore, we set up a test platform that allows the deployment of up to 14 colocated antennas simultaneously. In the signal acquisition section, we analyze track capability, signal-to-noise ratio (SNR) and code multipath error for eight different types of antennas. In the receiver noise estimation section, we investigate

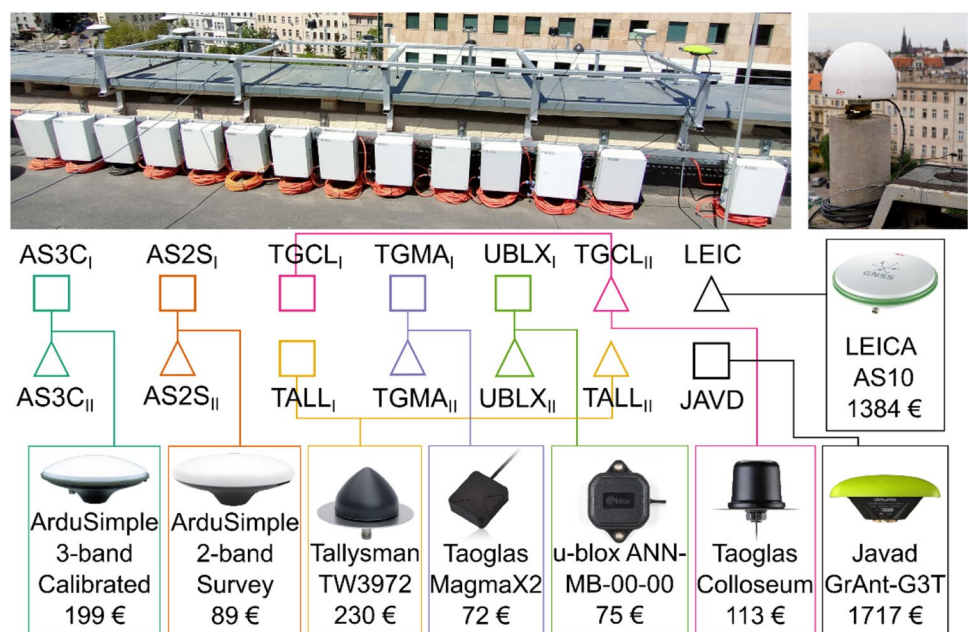
double differences of code and phase observations using a zero-baseline approach utilizing a GNSS splitter. The PCO determination part is dedicated to the estimation of frequency-specific PCOs for each GNSS. The following sections present multi-GNSS positioning results using double-difference (DD), PPP and PPP-AR techniques with null and estimated PCOs. In each section, a description of the methods is given followed by the corresponding results.

Test platform and GNSS instrumentation

In order to acquire the GNSS data from low-cost receivers, we perform a continuous measurement campaign, which takes place from July 5th to July 18th, 2022. We use 14 antennas and receivers setup on the roof of the Institute of Geodesy and Geoinformatics, Wrocław University of Environmental and Life Sciences, Poland, using the test platform located approximately 20 m from the International GNSS Service (IGS) WROC station (Fig. 1). To determine the reference coordinates of mounting points, we perform daily static measurements with geodetic-grade GNSS receivers simultaneously on four corner points and determine their horizontal coordinates with respect to the WROC station with the baseline processing using the Bernese 5.2 software (Dach et al. 2015). We measure horizontal distances between all neighboring points and determine reference coordinates of the inner points using the least squares adjustment. The vertical coordinates of all measured points were determined using precise leveling with respect to the WROC station. The estimated accuracy is 2 mm and 1 mm for horizontal and vertical components, respectively.

We use the in-house developed receivers equipped with the widely used low-cost high-precision GNSS module u-blox ZED-F9P and the microcomputer Raspberry Pi Zero W. The receivers track GPS L1 C/A and L2C, GLONASS L1OF and L2OF and Galileo E1 B/C and E5b and BeiDou B1I and B2I signals. The devices utilize proprietary software written in the Python programming language, enabling bidirectional communication between the microcomputer and the u-blox module. We store dual-frequency carrier-phase and code observations in the RINEX v.3 format with 30 s sampling rate and elevation mask of 3°. Due to software limitations, we reject observations from BeiDou. We connect 12 low-cost receivers to six pairs of low-cost antennas available on the market: ArduSimple AS-ANT2B-SUR-L1L2-25SMA-00 (AS2S, version with no NGC calibration), ArduSimple AS-ANT3B-CAL-L1256-SMATNC-01 (AS3C), Taoglas Colloseum (TGCL), Taoglas MagmaX2 (TGMA), Tallysman TW3972 (TALL) and u-blox ANN-MB-00-00 (UBLX) (Fig. 1). The two remaining receivers we connect to two geodetic-grade antennas, namely Leica AS10 (LEIC) and JAVAD GrAnt-G3T (JAVD), which allow for connection to receivers with lower output voltage. For antennas, such as UBLX, TGCL, TGMA and TALL, whose construction prevents factory centering as envisaged by the manufacturer, we develop and manufacture dedicated mounts using computerized numerical control (CNC) technology. These mounts facilitate precise centering at the measurement point. Only three low-cost antennas, i.e., AS3C, UBLX and TALL, clearly indicate the North direction. For AS2S and TGMA, we apply the convention of using the off-centered antenna cable attachment point as the north marker. For the TGCL antenna, the antenna cable

Fig. 1 Test platform with 14 low-cost GNSS receivers connected to 12 low-cost and two geodetic-grade GNSS antennas during the first measurement campaign



connector is centered at the bottom plate; thus, the manufacturers seem to assume null horizontal PCOs and no azimuth-dependent PCVs. Since all test antennas are colocated in open-sky conditions, and acquire observations simultaneously, we consider the comparison fair and equally affected by environmental effects.

Moreover, from May 26th to 28, 2023, we connect one AS3C antenna to four low-cost receivers through a GPS Networking ALDCBS1X8 active splitter and store 3 days of multi-GNSS observations for further analysis of signals' noises.

Signal acquisition

Due to the short distance between the WROC station and the setup test platform, the direct comparison of signals tracked by geodetic-grade and low-cost GNSS antennas is possible. We assume that colocated receivers should concurrently track the same satellites, and thus, a similar number of observations should be available. While WROC station uses multiple signal tracking modes, low-cost receivers are limited to GPS (C1C, L1C, C2L, L2L), GLONASS (C1C, L1C, C2C, L2C) and Galileo (C1C, L1C, C7Q, L7Q). There is no direct match for the second GPS frequency, so, as an exception, we use C2W and L2W from station WROC as a reference. For each GNSS constellation and frequency independently, we calculate the acquisition ratio defined as the percentage of observations acquired with low-cost receivers and observations available at geodetic-grade receiver connected to a high-end antenna, i.e., station WROC.

Results

We notice that acquisition ratios are similar for code and carrier-phase observations, but depend on GNSS and frequency; hence, we analyze results averaged for both types of observations over the two-week period (Fig. 2). For the first frequency, low-cost receivers achieve acquisition ratios exceeding 99% in most cases. Only two types of low-cost antennas have significantly lower ratios, i.e., TGCL with the lowest ratio of 89.6% for GLONASS and 95.5% for Galileo and TALL with a ratio equal to 96.4% for GLONASS. For the second frequency, there are major differences among GNSS constellations. For Galileo, the ratios are comparable or slightly lower than the ratios at the first frequency, i.e., for E1 and E5b the mean among all receivers was 99% and 97%, respectively. Again, both TGCL and one TALL antennas perform significantly worse than other antennas. Noticeably, for GPS and GLONASS the ratios for the second frequency are lower by up to 28% as compared to the first frequency. The average ratios are 71.4% and 85.7% for GPS

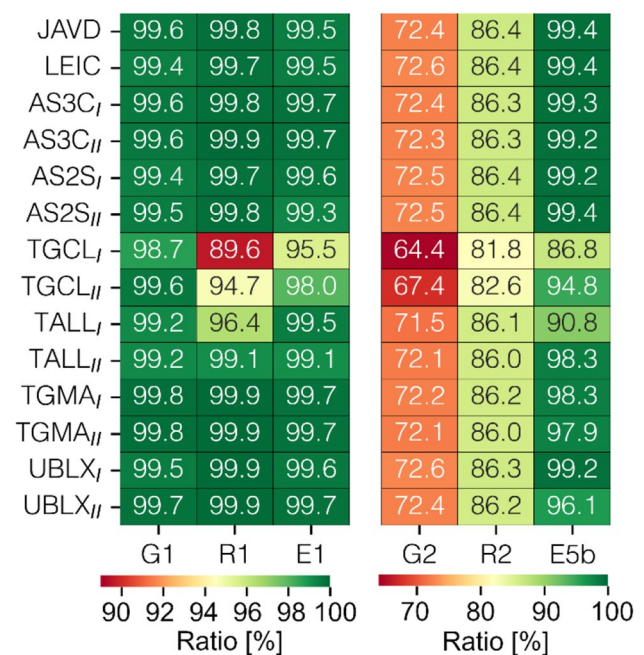
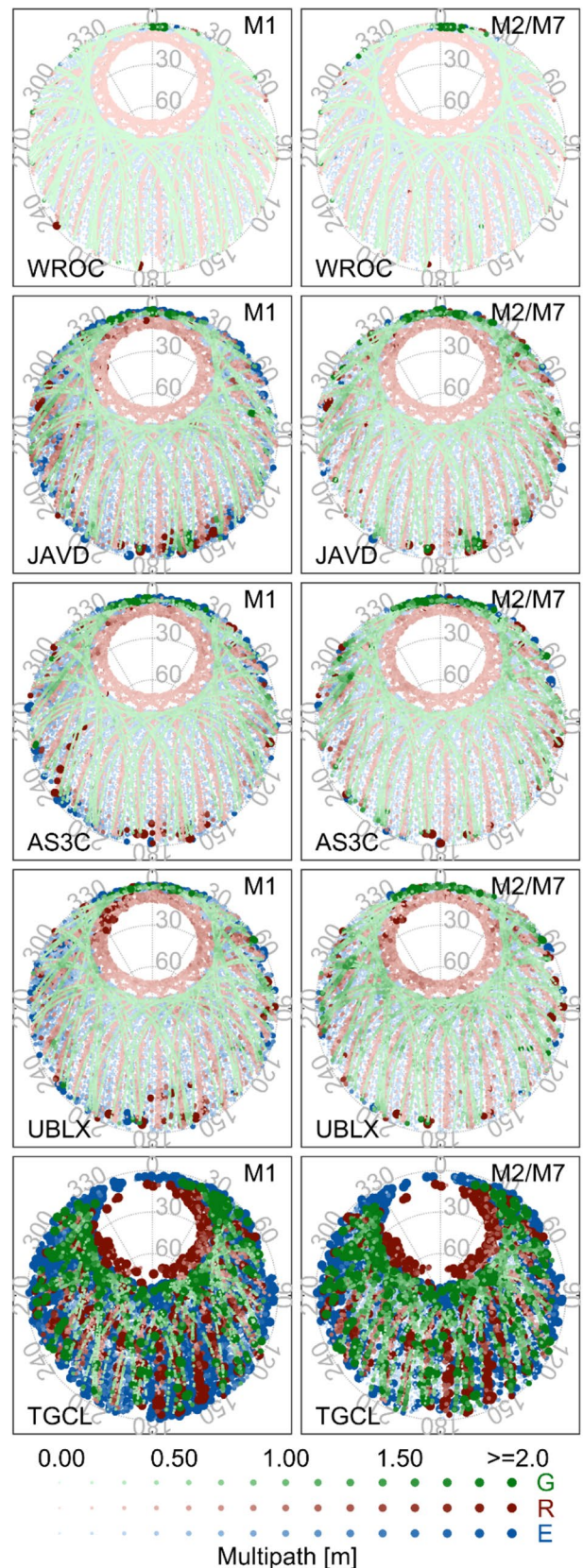


Fig. 2 Acquisition ratios between low-cost receivers and station WROC for the first (left) and the second (right) frequency

and GLONASS, respectively. Both TGCL antennas underperform, whereas the ratio for the TALL antenna is similar to ratios for other low-cost antennas.

Furthermore, we analyze the SNR and multipath parameters using the Anubis Free 3.3 software (Vaclavovic and Dousa 2015). The detailed procedure for calculating code multipath is presented in the user manual of the Anubis software (https://gnutsoftware.com/themes/gnut/assets/files/anubis_manual.pdf?v3). We notice that GPS and Galileo signals acquired by low-cost receivers are typically weaker than signals from WROC station by 3 dB-Hz to almost 9 dB-Hz (Fig. 3). For GLONASS, most low-cost antennas achieve similar SNR as station WROC, but it is rather due to the underperformance of station WROC, for which GLONASS SNRs are lower by c.a. 5 dB-Hz than for other GNSS. Whereas we observe a typical increase of the SNR with the increasing elevation angle, the two TGCL antennas do not reveal such characteristics, which we attribute to their helical construction (Narbudowicz 2021). We notice that various antennas have varying characteristics, but the differences between any two antennas of the same type remain at 1 dB-Hz level, except the TALL antennas, for which they reach up to 3.5 dB-Hz (GLONASS L1).

The code multipath analysis reveals a major increase in the multipath for both low-cost and geodetic-grade antennas connected to low-cost receivers compared to the high-grade receiver and antenna on station WROC (Fig. 4). For station WROC the multipath typically remains below 20 cm, whereas for low-cost antennas, signals coming from the same azimuth



and elevation are affected by multipath c.a. 5 times more (even 20 times more for TGCL antennas) for all GNSS. Multipath remains two times lower for the second frequency than for the first frequency, except low-elevation observations, for which the multipath on both frequencies is similar. The JAVD antenna connected to the low-cost receiver shows no significant difference in recorded multipath compared to the survey AS3C antenna, for which the results are at a similar level. However, both antennas exhibit noticeable distinctions when compared to the UBLX antenna. While there are no major differences between the majority of low-cost antennas, both TGCL antennas performed significantly worse with multipath frequently exceeding 2 m.

 Springer

Receiver noise estimation

Following Ruwisch et al. (2020), we form six possible combinations of four receivers taken two at a time. Using observations with ideally corresponding time stamps, we calculate double difference of code and phase observations as:

$$\nabla \Delta x = (x_m^{f,p} - x_m^{f,q}) - (x_n^{f,p} - x_n^{f,q}) = \varepsilon_{x_{mn}^{f,pq}} + N_{mn}^{f,pq} \quad (1)$$

where $\nabla \Delta x$ is the doubled differenced code or phase observation in meters or cycles, respectively, x is the measured code or phase observation in meters or cycles, respectively, m and n denote two receivers from pair, p and q denote two satellites from the same satellite's system, f is the frequency of observations, N is the ambiguity part (only for phase observation) and ε is the error of differenced observations. The ambiguity part is integer by nature; thus, the fractional part of the double-differenced carrier phases indicates the observation noise. However, due to frequency division multiple access (FDMA) in GLONASS, a linear fitting method is applied to reject unmodeled effects (Cai et al. 2016). Moreover, despite the exact time stamps of observations in a pair of RINEX files, due to the low-quality internal clocks of low-cost receivers, we assume a mis-synchronized reception. Since it is not eliminated by double differencing, it affects the ambiguity part, so we subtract it using the linear fitting for each continuous arc of observations.

We notice that the noise level of code observations is GNSS and frequency dependent (Fig. 5, top). For the first frequency, it ranges from 0.5 m to approximately 1 m, being typically the lowest for Galileo and the largest for GLONASS. For pseudoranges recorded at the second frequency, we observe a significant reduction of the noise level for Galileo observation, i.e., it remains below 0.4 m. There is a slight improvement also for GPS pseudoranges, but very limited or none for GLONASS. For GPS L1/L2 and Galileo E1/E5b, the noise of carrier-phase observations does not exceed 5 mm (Fig. 5, bottom). For GLONASS, we observe that the noise level varies over time, especially for the L2OF. The noise of observations is nearly twice as large as for other GNSS and at times exceeds 10 mm and 20 mm for the first and second frequency, respectively.

For each pair of receivers, we calculate standard deviation of noise among the entire test period, independently for each GNSS, observation type (code or carrier phase) and frequency (Fig. 6), and consider it as a reliable measure of the observation noise. We find that the noise for GPS and Galileo is consistent across all receiver pairs. The average for GPS code observations is 0.25 m and 0.20 m for C1 and C2, respectively. For Galileo the corresponding values are lower, i.e., 0.20 m and 0.12 m, respectively. For GLONASS, there are relatively large differences between pairs and the noise varies from 0.24 to 0.40 m, with the average

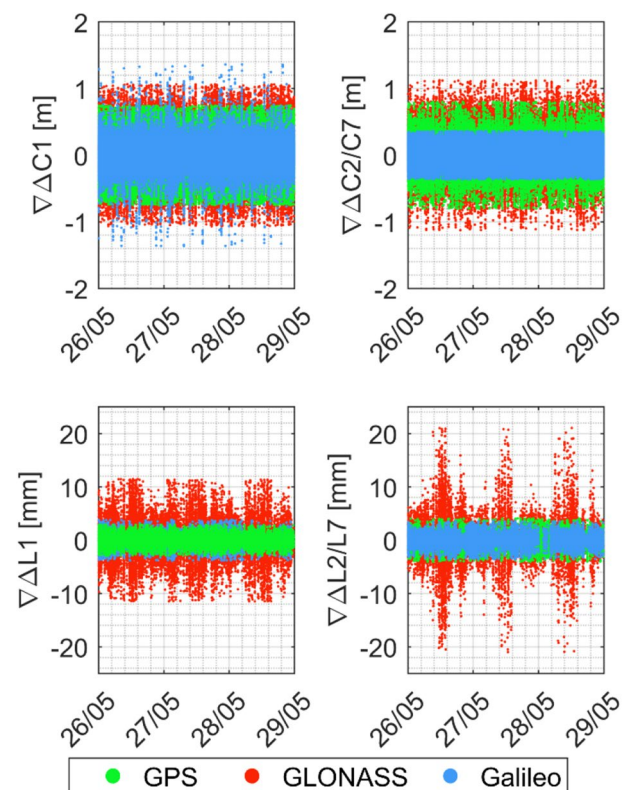


Fig. 5 Double-differenced code (top) and carrier-phase (bottom) observations for the first (left) and the second (right) frequency, GNSS receivers BX03-BX08

σ_{C1} [m]				$\sigma_{C2/C7}$ [m]			
BX03-BX08	0.23	0.30	0.17	0.19	0.28	0.12	
BX03-BX12	0.24	0.25	0.21	0.20	0.40	0.13	
BX03-BX15	0.25	0.32	0.19	0.20	0.32	0.12	
BX08-BX12	0.24	0.35	0.21	0.20	0.31	0.12	
BX08-BX15	0.25	0.24	0.21	0.19	0.25	0.12	
BX12-BX15	0.27	0.38	0.22	0.20	0.28	0.12	
	G	R	E	G	R	E	
σ_{L1} [mm]				$\sigma_{L2/L7}$ [mm]			
BX03-BX08	0.9	3.0	1.2	1.3	3.7	1.1	
BX03-BX12	0.9	3.6	1.2	1.4	3.7	1.1	
BX03-BX15	0.9	2.5	1.2	1.4	3.8	1.1	
BX08-BX12	0.9	4.2	1.2	1.3	4.0	1.1	
BX08-BX15	0.9	3.3	1.2	1.3	3.7	1.1	
BX12-BX15	0.9	4.1	1.2	1.3	4.6	1.1	
	G	R	E	G	R	E	

Fig. 6 Standard deviation of code (top) and carrier-phase (bottom) observation noises at first (left) and second (right) frequency categorized by GNSS and receivers' pair

of 31 mm for both frequencies. The carrier-phase noise is the lowest for GPS L1, i.e., 0.9 mm on average, and slightly larger for GPS L2 and both Galileo frequencies, reaching up to 1.4 mm. For GLONASS, the average noise of carrier-phase observations is 3.5 mm and 3.0 mm for the first and second frequency, respectively. The significantly larger level of noise for GLONASS code and carrier-phase observation we justify by the frequency spacing due to the FDMA.

PCO determination

We use the Bernese 5.2 software (Dach et al. 2015) and the baseline strategy to estimate daily coordinates of low-cost antennas using single-frequency and single GNSS observations. In this way, for each antenna, we determined electrical phase centers for each system and frequency independently with respect to the base station WROC. We compare the daily values against reference coordinates of the physical center points of the test platform and determine the corresponding differences in the North, East and Up directions. Although these differences were estimated in the relative mode, through the use of individual calibration model for base station WROC, we consider them as absolute. Due to a very good agreement between daily solutions, we determine PCOs as:

$$x_s^f = \frac{\sum \Delta x_{s,t}^f \cdot \sigma(\Delta x_{s,t}^f)}{\sum \sigma(\Delta x_{s,t}^f)} \quad (2)$$

where x is the calculated PCO in North, East and Up, respectively, Δx is the corresponding daily difference between estimated and reference position, f is the frequency, s is the satellite system, t indicates the day and σ is the a posteriori error of the estimated position component. For validation purposes, we use the same strategy to determine PCOs of two geodetic-grade antennas, i.e., JAVD and LEIC, which have individual and model calibrations, respectively. We also compare estimated PCOs for AS3C antennas against the National Geodetic Survey (NGS) model for GPS.

Figure 7 presents the daily differences obtained for the Galileo system, as a representative example. The differences in the horizontal and vertical components are antenna- and frequency dependent. For the two geodetic-grade antennas, the differences oscillate from -6 to $+9$ mm in the horizontal component and -9 mm to $+8$ mm in the vertical component, confirming that the applied method is accurate to sub-cm level, despite the use of a low-cost GNSS receiver. For the AS3C antennas, the estimated PCOs differ from the NGS model by up to 8 mm and 13 mm, for the horizontal and vertical components, respectively.

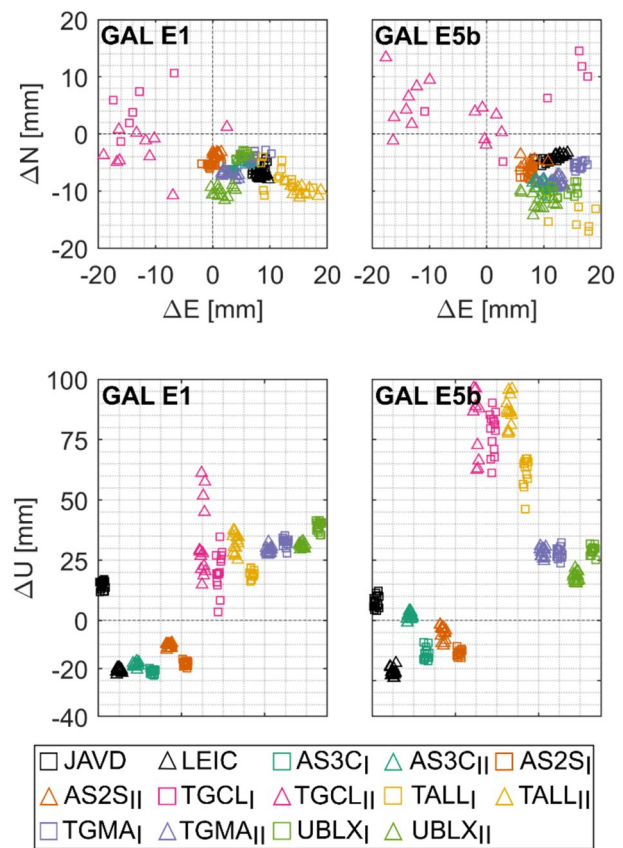


Fig. 7 Coordinate differences in horizontal (left) and vertical (right) components for the first (top) and second (bottom) frequency of the Galileo system

For each antenna, the repeatability of daily differences is at the level of single millimeters, which proves the high precision of the applied method. However, this is not the case for the two TGCL and the two TALL antennas, for which the daily results vary among each other by tens of millimeters, both in the horizontal and vertical components. The determined horizontal PCOs are typically on a few mm level and agree between two antennas of the same type. However, for the vertical component PCOs are much larger and differ by up to 25 mm (Table 1). Such a divergence excludes the possibility of using a low-cost antenna for precise GNSS leveling unless individual calibration is provided. In light of the above, we decide not to calculate model-averaged PCOs, but to use antenna-specific PCOs. We notice offsets in North and East components are typically below 5 mm, with a few offsets reaching up to 10 mm. However, the vertical offset for the majority of tested antennas is positive and reaches up to 82 mm. The PCO differences between frequencies are marginal for the horizontal components, while for the vertical component, they reach up to 38 mm, 54 mm and 41 mm for GPS, GLONASS and Galileo, respectively.

Table 1 Estimated vertical PCOs [mm]

[mm]	G1	G2	R1	R2	E1	E5b
JAVD	16.6	29.6	14.4	27.5	14.5	26.1
LEIC	50.1	57.9	51.5	55.5	49.8	54.9
AS3C _I	48.3	38.2	48.5	41.3	47.6	32.0
AS3C _{II}	51.0	51.1	51.8	52.3	50.3	47.6
AS2S _I	40.5	40.9	41.7	38.8	39.7	39.0
AS2S _{II}	48.4	51.0	47.3	52.0	47.0	47.3
UBLX _I	−0.2	17.3	−0.3	20.7	−1.8	15.8
UBLX _{II}	−8.3	14.9	−9.6	13.2	−9.9	4.6
TGMA _I	3.0	10.0	−7.6	13.7	−0.1	5.5
TGMA _{II}	−3.2	10.4	−7.6	15.0	−3.2	6.0
TGCL _I	23.2	—	—	—	−3.7	−60.2
TGCL _{II}	−2.7	−39.5	—	−45.8	8.3	−44.2
TALL _I	−2.2	−46.8	−2.1	−30.3	−2.9	−52.6
TALL _{II}	8.2	−33.8	16.3	−25.7	10.0	−27.3

We also check the consistency of PCOs determined with various GNSS for the corresponding frequencies. Neglecting the two TGCL and two TALL antennas, the L1 PCOs determined with GPS and Galileo agree better than 2 mm, but the differences for GLONASS L1 against GPS L1 reach up to 7 mm and 10 mm for the horizontal and vertical components, respectively. For L2, PCOs between GPS and GLONASS differ up to 7 mm and 5 mm, respectively. The PCOs for Galileo E5b vary from PCOs for GPS L2 by up to 4 mm and 10 mm, respectively. Such results imply that the adaptation of missing PCOs from other systems and/or frequencies, which is a common case for low-cost antennas, is invalid and leads to inconsistent processing of multi-GNSS observations.

Positioning results

We perform four reprocessing of our data, i.e., (1) DD with null PCO (DDnull), (2) DD with determined PCO (DDpco), (3) PPP with null PCO (PPPnull) and (4) PPP with determined PCO (PPPpco). Both DD reprocessings are performed with the Bernese 5.2 software, and both PPP reprocessings are performed with the GNSS-WARP software (Hadas and Hobiger 2021). In all cases we process multi-GNSS observations, i.e., GPS + GLONASS + Galileo, we apply null PCV model, use multi-GNSS clock and orbits products provided by Center for Orbit Determination in Europe (CODE) as well as apply troposphere parameters obtained from the Vienna Mapping Functions 1 (VMF1, Boehm et al. 2006). The resulting daily coordinates are compared against the reference ones.

Multi-GNSS DD.

Before applying the PCO, the multi-GNSS DD daily solutions, i.e., DDnull, occurred to be highly precise for most

stations, i.e., the horizontal repeatability of the coordinates is at the level of single millimeters (Fig. 8, top left). Since the results obtained for stations equipped with both TGCL and one TALL antennas are highly imprecise and inaccurate, they will no longer be discussed in this section, but the results are presented in the figures. For the other stations, the estimated coordinates are typically biased toward the South and East directions by up to 10 mm. Moreover, we

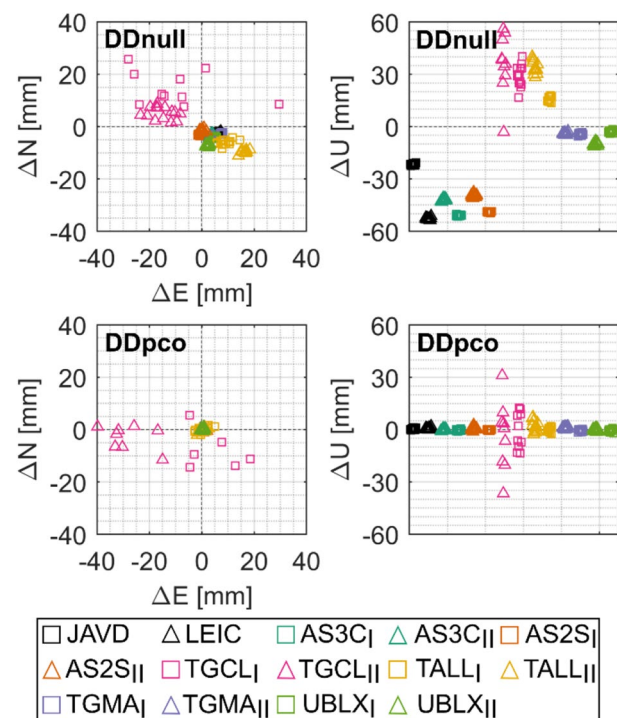


Fig. 8 Horizontal (left) and vertical (right) differences of daily positions from the DD solutions with null PCOs (top) and with the determined PCOs (bottom)

notice that most stations equipped with the same antenna type reveal consistent horizontal offsets. For the vertical component, we reach a sub-centimeter precision (Fig. 8, top right). The vertical biases vary from -55 to $+60$ mm. More important, for some stations equipped with the same antenna type, i.e., AS3C, AS2S and UBLX, the offsets are not consistent by up to 9 mm.

In the corresponding DD solution with PCO applied, i.e., in DDpco, we notice a clear improvement of accuracy for both the horizontal (Fig. 8, bottom right) and vertical (Fig. 8, bottom left) components. The horizontal and vertical differences do not exceed 2 mm and 3 mm, respectively. Consistent DDpco results are obtained among stations equipped with the same antenna type. The repeatability of coordinates estimated with low-cost antennas remains at a similar level to coordinates estimated with geodetic-grade antennas, i.e., standard deviations do not exceed 0.6 and 1.0 mm for the horizontal and vertical components, respectively.

Multi-GNSS PPP

The multi-GNSS PPP solutions with null PCOs, i.e., PPPnull (Fig. 9, top), are less precise and less accurate than DDnull. The results obtained for stations equipped with both TGCL and one TALL antennas are so highly imprecise and inaccurate, that only individual solutions are presented in the figure, whereas others exceed the scale. Therefore, results from these three antennas will no longer be discussed in

this section. PPPnull allows us to reach precision better than 20 mm in the horizontal and vertical components, with sub-cm horizontal offsets and vertical offsets varying from -77 to $+32$ mm. Most stations equipped with the same antenna type reveal consistent horizontal offsets and vertical offsets varying at the sub-cm level.

Application of determined multi-GNSS PCOs to PPP solutions increases both the accuracy and the precision of estimated coordinates. All solutions are shifted westward by 6 mm on average and we obtain sub-cm precision, which we justify by the limitations of the PPP technique. In the vertical component, the precision is not improved with respect to the PPPnull solutions, but offsets are dramatically reduced for all antennas but still vary from -15 to $+30$ mm. Again we find sub-cm inconsistencies between solutions obtained with stations equipped with the same type of antenna.

Although PPPpco (Fig. 9, bottom) solutions are not as good as DDpco solutions, it should be noted that DDpco is obtained with the same software and analogous strategy that we use for PCO estimation, which is not the case for PPPpco.

PPP with ambiguity resolution

Since PPP-AR requires not only precise satellite and clock correction, but also code and phase biases, we use real-time products from CNES, which we find to be the only analysis center providing the set of products being fully consistent with the tracked signal (in RINEX 3 notation GPS: C1C, C2L, L1C, L2L; Galileo: C1C, C7Q, L1C, L7Q). We perform four different variants of simulated real-time data processing, i.e., (1) PPP with null PCO (PPPnull), (2) PPP with determined PCO (PPPpco), (3) PPP-AR with null PCO (ARnull) and (4) PPP-AR with determined PCO (ARpco). We process GPS and Galileo observations using the G-Nut/ Geb Pro software. Receiver signal biases are eliminated through between-satellites single-differences (Vaclavovic and Nesvadba 2020). Integer ambiguities are resolved with the least-squares ambiguity decorrelation adjustment (LAMBDA) method incorporating the float ambiguity solution from the Kalman filter as input.

For the ARpco variant, the ambiguity fixing rate, defined as the ratio of the number of fixed epochs to the number of total epochs, oscillates around 99% for all low-cost receivers except those equipped with TALL and TGCL antennas, for which the fixing rates are 98% and 5%, respectively. This is comparable with the fixing rate of 99.2% obtained for the colocated geodetic-grade station WROC. The fixing rate of the ARnull variant was lower by c.a. 0.5%. We notice that PPP solutions with the determined PCOs are slightly more accurate than respective solutions with null PCOs, and the ambiguity resolution improves the repeatability,

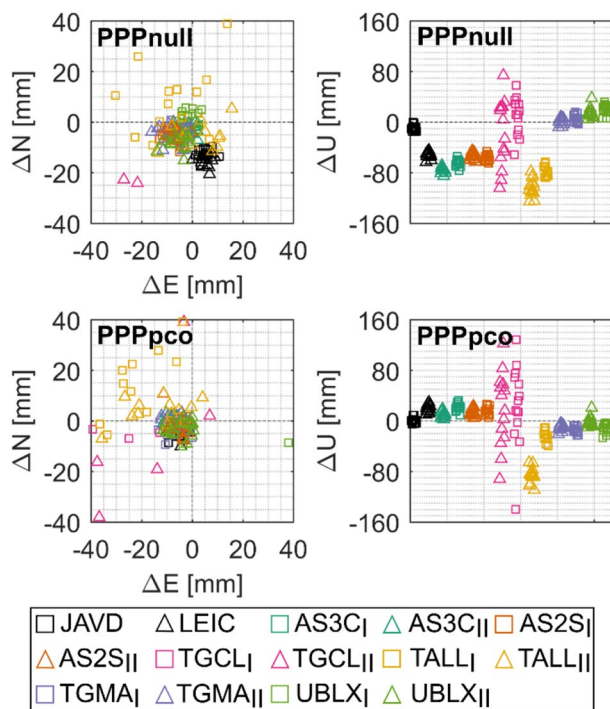


Fig. 9 Horizontal (left) and vertical (right) differences of daily positions from the PPP solutions with null PCOs (top) and with the determined PCOs (bottom)

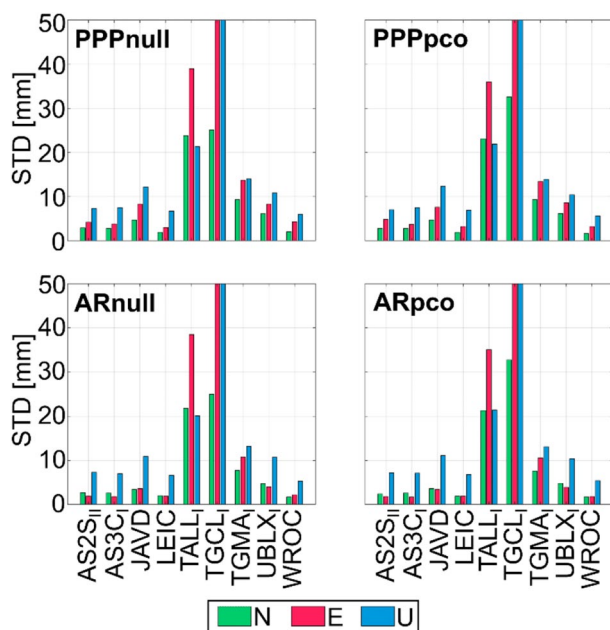


Fig. 10 Repeatability of the North, East and Up coordinates components of float PPP (top) and PPP-AR (bottom) solutions with null (left) and determined (right) PCOs

i.e., standard deviation of coordinates, especially of the East component (Fig. 10).

The most accurate results were obtained from stations equipped with low-cost AS2S and AS3C antennas, and are comparable to results obtained with the geodetic-grade LEIC antenna. We evaluated in terms of convergence time to achieve 5 cm horizontal/vertical accuracy. Convergence is considered achieved when the horizontal/vertical standard deviation of at least 10 consecutive epochs (5 min) did not exceed 5 cm. The determined PCOs allow for slightly faster convergence time, while the ambiguity resolution improved the convergence time except for the station equipped with the UBLX antenna (Fig. 11). Again, TALL and TGCL antennas underperform, while the fastest convergence is obtained with AS2S, AS3C and LEIC antennas.

Conclusions

Antennas have been identified as the main limiting hardware factor for precise positioning applications with low-cost receivers. Therefore, we compare the performance of six types of low-cost antennas with two geodetic-grade antennas in terms of signal acquisition, SNR and multipath characteristics. We estimate receiver noise and determine PCOs for individual constellation and frequencies. Finally, we investigate the accuracy and precision of GNSS positioning with DD and PPP technique. For the latter, we investigate the

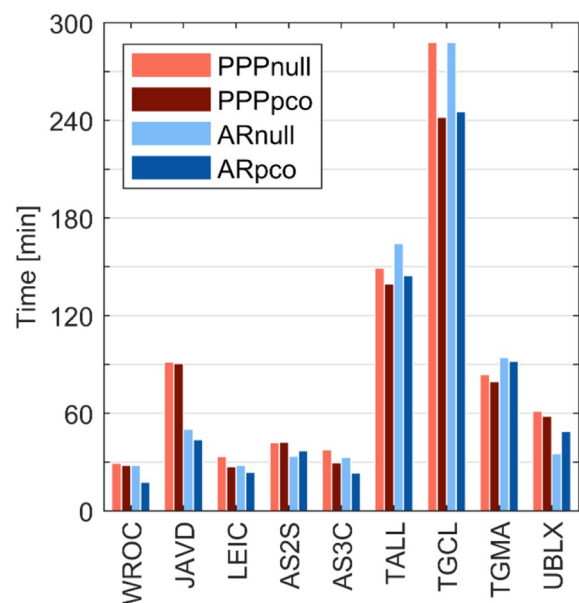


Fig. 11 Average time required to achieve 5 cm horizontal/vertical accuracy (95%) of float PPP and PPP-AR solutions with null and determined PCOs

feasibility of doing PPP-AR. We reveal clear differences in the performance of the test antennas, which are as follows.

- The acquisition of GPS L1, Galileo E1 and E5b signals with low-cost antennas is similar to geodetic-grade antennas, which is not the case for GPS L2 and GLONASS L2. Both tested TGCL helical antennas acquire significantly less observations than other test antennas, especially for the GLONASS L1 frequency.
- Helical antennas underperform in terms of SNR characteristics, whereas the other antennas acquire signals weaker by c.a. 3 dB-Hz compared with a geodetic-grade antennas.
- Low-cost antennas appear to be vulnerable to the multipath effect; for most test antennas, it is on average 5 times larger than for a geodetic-grade antenna.
- Antenna PCOs vary significantly between frequencies and constellations; moreover, they do not agree between two antennas of the same type by up to 25 mm in the vertical component.

Moreover, we notice that the noise of signals tracked by low-cost receivers is constellation and frequency dependent. For pseudoranges, the noise varies from 0.12 m for Galileo E5b to over 0.30 m for GLONASS L1 and L2, whereas for carrier-phase observations, it oscillates around 1 mm for both GPS and Galileo frequencies, but exceeds 3 mm for both GLONASS frequencies. Such results indicate the need of redefinition of the stochastic model, i.e., the altering the multi-GNSS observation weighting scheme.

Our results confirm that selection of low-cost antenna for a low-cost GNSS receiver is of great importance in precise positioning applications. Although the horizontal coordinates can be accurately estimated with the majority of antennas, the accurate determination of station height requires individual determination of PCO. The proposed field-calibration method, that allows to determine the offsets with sub-centimeter accuracy for all GNSS constellations and individual frequencies, improves the multi-GNSS positioning performance, i. e.:

- The accuracy of daily static DD solutions is better than 2 mm and 3 mm for the horizontal and vertical components, respectively,
- In daily static PPP solutions, sub-cm accuracy is obtained for horizontal coordinates, whereas vertical offsets vary from -15 to $+30$ mm.

Positioning results that we obtain with AS2S, AS3C and TGMS antennas are the best among low-cost antennas and are similar to results obtained with both tested geodetic-grade antennas. However, it is expected that the differences are more highlighted when working in adverse conditions.

Last but not least, we demonstrate that PPP-AR is possible also with low-cost GNSS receivers and antennas. AR improves the convergence time and repeatability, i.e., precision, of estimated coordinates. The AR success rate that we achieve with AS2S and AS3C antennas exceeds 99% and is comparable to both tested geodetic-grade antennas.

Acknowledgements This work was supported by the National Science Centre, Poland (NCN) grant 2020/39/I/ST10/01318. The article is part of a PhD dissertation titled “New fields for the use of low-cost GNSS receivers for real-time monitoring of natural and anthropogenic phenomena and hazards”, prepared during Doctoral School at the Wrocław University of Environmental and Life Sciences. The APC/BPC is financed by Wrocław University of Environmental and Life Sciences.

Author contributions G.M. was responsible for calculations, formal analysis, resources, data curation, visualization and writing the original draft. T.H. contributed to conceptualization, methodology, supervision, funding acquisition and the review and editing of the manuscript. J.N. handled AR calculations and wrote the AR section, as well as contributed to the review process.

Data availability All RINEX files from the low-cost receivers used in the experiments are available at <https://doi.org/10.5281/zenodo.10209844>.

Declarations

Conflict of interest The authors declare no competing interests.

Ethical approval and consent to participate Not applicable.

Consent for publication Not applicable.

Open Access This article is licensed under a Creative Commons Attribution 4.0 International License, which permits use, sharing, adaptation, distribution and reproduction in any medium or format, as long as you give appropriate credit to the original author(s) and the source, provide a link to the Creative Commons licence, and indicate if changes were made. The images or other third party material in this article are included in the article's Creative Commons licence, unless indicated otherwise in a credit line to the material. If material is not included in the article's Creative Commons licence and your intended use is not permitted by statutory regulation or exceeds the permitted use, you will need to obtain permission directly from the copyright holder. To view a copy of this licence, visit <http://creativecommons.org/licenses/by/4.0/>.

References

- Biagi L, Grec F, Negretti M (2016) Low-cost GNSS receivers for local monitoring: experimental simulation, and analysis of displacements. *Sensors* 16(12):2140. <https://doi.org/10.3390/s16122140>
- Boehm J, Werl B, Schuh H (2006) Troposphere mapping functions for GPS and very long baseline interferometry from European Centre for Medium-Range Weather Forecasts operational analysis data: troposphere mapping functions from ECMWF. *J Geophys Res Solid Earth*. <https://doi.org/10.1029/2005JB003629>
- Bojorquez-Pacheco N, Romero-Andrade R, Trejo-Soto ME, Hernández-Andrade D, Nayak K, Vidal-Vega AI, Arana-Medina AI, Sharma G, Acosta-Gonzalez LE, Serrano-Agila R (2023) Performance evaluation of single and double-frequency low-cost GNSS receivers in static relative mode. *Geod Vestn* 67(02):235–248. <https://doi.org/10.15292/geodetski-vestnik.2023.02.235-248>
- Cai C, He C, Santerre R, Pan L, Cui X, Zhu J (2016) A comparative analysis of measurement noise and multipath for four constellations: GPS, BeiDou, GLONASS and Galileo. *Surv Rev* 48(349):287–295. <https://doi.org/10.1179/1752270615Y.0000000032>
- Cina A, Piras M (2015) Performance of low-cost GNSS receiver for landslides monitoring: test and results. *Geomat Nat Hazards Risk* 6(5–7):497–514. <https://doi.org/10.1080/19475705.2014.889046>
- Correa Muñoz NA, Cerón-Calderón LA (2018) Precision and accuracy of the static GNSS system for surveying networks used in Civil Engineering. *Ing E Investig* 38(1):52–59
- Dach R, Lutz S, Walser P, Fridez P (2015) Bernese GNSS software, version 5.2. AIUB-Astronomical Institute, University of Bern, Bern, Switzerland
- Garrido-Carretero MS, De Lacy-Pérez De Los Cobos MC, Borque-Arancón MJ, Ruiz-Armenteros AM, Moreno-Guerrero R, Gil-Cruz AJ (2019) Low-cost GNSS receiver in RTK positioning under the standard ISO-17123-8: a feasible option in geomatics. *Measurement* 137:168–178. <https://doi.org/10.1016/j.measurement.2019.01.045>
- Hadas T, Hobiger T (2021) Benefits of using galileo for real-time GNSS meteorology. *IEEE Geosci Remote Sens Lett* 18(10):1756–1760. <https://doi.org/10.1109/LGRS.2020.3007138>
- Hamza V, Stopar B, Ambrožič T, Sterle O (2021a) Performance evaluation of low-cost multi-frequency gnss receivers and antennas for displacement detection. *Appl Sci* 11(14):6666. <https://doi.org/10.3390/app11146666>
- Hamza V, Stopar B, Sterle O (2021b) Testing the performance of multi-frequency low-cost GNSS receivers and antennas. *Sensors* 21(6):2029. <https://doi.org/10.3390/s21062029>
- Hamza V, Stopar B, Sterle O, Pavlovčič-Prešeren P (2023) Low-cost dual-frequency GNSS receivers and antennas for surveying in

- urban areas. *Sensors* 23(5):2861. <https://doi.org/10.3390/s23052861>
- Han X, Kim HJ, Jeon CW, Moon HC, Kim JH (2017) Development of a low-cost GPS/INS integrated system for tractor automatic navigation. *Int J Agric Biol Eng* 10(2):123–131. <https://doi.org/10.3965/j.ijabe.20171002.3070>
- Jagoda M (2021) Determination of motion parameters of selected major tectonic plates based on GNSS station positions and velocities in the ITRF2014. *Sensors* 21(16):5342. <https://doi.org/10.3390/s21165342>
- Kazmierski K, Dominiak K, Marut G (2023) Positioning performance with dual-frequency low-cost GNSS receivers. *J Appl Geod* 17(3):255–267. <https://doi.org/10.1515/jag-2022-0042>
- Komac M, Holley R, Mahapatra P, Van Der Marel H, Bavec M (2015) Coupling of GPS/GNSS and radar interferometric data for a 3D surface displacement monitoring of landslides. *Landslides* 12(2):241–257. <https://doi.org/10.1007/s10346-014-0482-0>
- Krietemeyer A, Van Der Marel H, Van De Giesen N, Ten Veldhuis M-C (2020) High quality zenith tropospheric delay estimation using a low-cost dual-frequency receiver and relative antenna calibration. *Remote Sens* 12(9):1393. <https://doi.org/10.3390/rs12091393>
- Krietemeyer A, Van Der Marel H, Van De Giesen N, Ten Veldhuis M-C (2022) A field calibration solution to achieve high-grade-level performance for low-cost dual-frequency GNSS receiver and antennas. *Sensors* 22(6):2267. <https://doi.org/10.3390/s22062267>
- Martín A, Anquela AB, Dimas-Pagés A, Cos-Gayón F (2015) Validation of performance of real-time kinematic PPP. A possible tool for deformation monitoring. *Measurement* 69:95–108. <https://doi.org/10.1016/j.measurement.2015.03.026>
- Marut G, Hadas T, Kaplon J, Trzcina E, Rohm W (2022) Monitoring the water vapor content at high spatio-temporal resolution using a network of low-cost multi-GNSS receivers. *IEEE Trans Geosci Remote Sens* 60:1–14. <https://doi.org/10.1109/TGRS.2022.3226631>
- Narbudowicz A (2021) Antenna technology for GNSS. *GPS and GNSS Technology in Geosciences*. Elsevier, Amsterdam, pp 99–117
- Nie Z, Zhang R, Liu G, Jia Z, Wang D, Zhou Y, Lin M (2016) GNSS seismometer: seismic phase recognition of real-time high-rate GNSS deformation waves. *J Appl Geophys* 135:328–337. <https://doi.org/10.1016/j.jappgeo.2016.10.026>
- Odolinski R, Teunissen PJG (2020) Best integer equivariant estimation: performance analysis using real data collected by low-cost, single-and dual-frequency, multi-GNSS receivers for short-to long-baseline RTK positioning. *J Geod* 94(9):91. <https://doi.org/10.1007/s00190-020-01423-2>
- Paziewski J, Sieradzki R, Baryla R (2019) Signal characterization and assessment of code GNSS positioning with low-power consumption smartphones. *GPS Solut* 23(4):98. <https://doi.org/10.1007/s10291-019-0892-5>
- Romero-Andrade R, Trejo-Soto ME, Vázquez-Ontiveros JR, Hernández-Andrade D, Cabanillas-Zavala JL (2021a) Sampling rate impact on precise point positioning with a low-cost GNSS receiver. *Appl Sci* 11(16):7669. <https://doi.org/10.3390/app11167669>
- Romero-Andrade R, Trejo-Soto ME, Vega-Ayala A, Hernández-Andrade D, Vázquez-Ontiveros JR, Sharma G (2021b) Positioning evaluation of single and dual-frequency low-cost GNSS receivers signals using ppp and static relative methods in urban areas. *Appl Sci* 11(22):10642. <https://doi.org/10.3390/app112210642>
- Ruwisch F, Jain A, Schön S (2020) Characterisation of GNSS carrier phase data on a moving zero-baseline in urban and aerial navigation. *Sensors* 20(14):4046. <https://doi.org/10.3390/s20144046>
- Skoglund M, Petig T, Vedder B, Eriksson H, Schiller EM (2016) Static and dynamic performance evaluation of low-cost RTK GPS receivers. In: 2016 IEEE Intelligent Vehicles Symposium (IV). IEEE, Gotenburg, Sweden, pp 16–19
- Stepniak K, Paziewski J (2022) On the quality of tropospheric estimates from low-cost GNSS receiver data processing. *Measurement* 198:111350. <https://doi.org/10.1016/j.measurement.2022.111350>
- Takatsu T, Yasuda A (2008) Evaluation of RTK-GPS performance with low-cost single-frequency GPS receivers. Tokyo
- Vaclavovic P, Dousa J (2015) G-Nut/Anubis: open-source tool for multi-GNSS data monitoring with a multipath detection for new signals, frequencies and constellations. In: Rizos C, Willis P (eds) IAG 150 Years. Springer International Publishing, Cham, pp 775–782
- Vaclavovic P, Nesvadba O (2020) Comparison and assessment of float, fixed, and smoothed precise point positioning. *Acta Geodyn Geomater* 17(3):329–340. <https://doi.org/10.13168/AGG.2020.0024>
- Vaquero-Martínez J, Antón M (2021) Review on the role of GNSS meteorology in monitoring water vapor for atmospheric physics. *Remote Sens* 13(12):2287. <https://doi.org/10.3390/rs13122287>
- Wielgocka N, Hadas T, Kaczmarek A, Marut G (2021) Feasibility of using low-cost dual-frequency GNSS receivers for land surveying. *Sensors* 21(6):1956. <https://doi.org/10.3390/s21061956>
- Yasyukevich YV, Kiselev AV, Zhivetiev IV, Edemskiy IK, Syrovatskii SV, Maletckii BM, Vesnin AM (2020) SIMuRG: system for ionosphere monitoring and research from GNSS. *GPS Solut* 24(3):69. <https://doi.org/10.1007/s10291-020-00983-2>
- Zhang L, Schwieger V (2018) Investigation of a L1-optimized choke ring ground plane for a low-cost GPS receiver-system. *J Appl Geod* 12(1):55–64. <https://doi.org/10.1515/jag-2017-0026>

Publisher's Note Springer Nature remains neutral with regard to jurisdictional claims in published maps and institutional affiliations.



Grzegorz Marut received his MSc in geoinformatics from Wrocław University of Environmental and Life Sciences (UPWr), Poland in 2021 and currently is a Ph.D. student. His main tasks include development of novel models for processing GNSS observations from low-cost receivers. His master's thesis was awarded by the Polish Space Agency and the Polish Ministry of Development and Technology.



Tomasz Hadas received his Ph.D. in satellite geodesy in 2015 and is currently an associate professor at UPWr, Poland. He is the co-author of the GNSS-WARP software for multi-GNSS data processing and focuses on real-time precise positioning algorithms and troposphere monitoring, as well as on the various applications of low-cost GNSS receivers in geomatics.



Jakub Nosek is a Ph.D. candidate at Brno University of Technology, Department of Geodesy. He received his M.Sc. degree in geodesy at this university in 2020. Since 2021, he has worked at Geodetic Observatory Pecny. His research interests involve multi-GNSS and multi-frequency PPP-AR.